Reduced Time Domain Behavioral Model of Three-Wire Shielded Power Cables

Ali Krim, Abderrazak Lakrim and Driss Tahri

Abstract**—**To quantify effectively the electromagnetic interference levels in a motor drive system, we have to build up a precise high frequency model of the power cable between the converter and the motor. In this context, this paper proposes a model of three conductors shielded power cables in time and frequency domain. This model takes into account all electromagnetic phenomena that occur in the cable when it is under a rapid variation of current and voltage. The rotational symmetry of the cable has been exploited to decouple its admittance matrix. Then, the frequency evolution of the admittance matrix eigenvalues has been approximated by using the vector-fitting tool. Thus, we obtain a behavioral model of the cable that is easy to convert to the time domain. Our approach has been validated by comparing the frequency and time responses of our model with those of a cascaded cell model, which is widely used in the literature.

Keywords**—**Time domain model, shielded power cables, per unit length parameters, admittance matrix, ANSYS Simplorer model.

I. Introduction

TO reduce the maintenance cost, increase safety and protect the environment, industrial systems have become increasingly more electric. This transition has been accompanied by the increased use of static converters. These last characterized by their high-performances, cost-effective can control the speed of electric motors. These converters are formed by electronic switches, which operate in commutation mode. The voltage and current variation due to the switching of these power transistors causes many EMC (Electromagnetic Compatibility) problems. The high-frequency interference generated from the converter propagates through the cable in differential and common mode and can cause significant damage [1]. Indeed, we will have a reflection of the electric field at the end of the cable because of the impedances mismatch. This reflection leads to an overvoltage at the load terminals [2]. In order to estimate these voltage peaks or to propose a filtering solution one must first have a model, which represents the cable under these conditions of use. In addition, this model must be precise and convergent.

Several research works of modeling energy cables have been presented in the literature [3]-[4] and [5]. The conventional method is to subdivide the cable into several parts. Each part is formed by a RLGC elementary cell [5]. The techniques for calculating the cable per unit length (p.u.l) parameters have been extensively discussed in the literature. The simplest and fastest technique is the analytical formulation [6]. However, it is limited to regular geometries and does not take into account the proximity effect. On the other hand, numerical methods treat the general case and are more reliable to determine these parameters [7]. Furthermore, finite element methods have grown considerably in recent decades because of their precision [8]. To model the frequency dependence of the p.u.l parameters, ladder networks have been widely used. Another technique that achieves this goal is to approximate the longitudinal impedance of the cable's cell with the vector-fitting tool [9].

The accuracy of the cascaded cell model depends strongly on the number of cells chosen per meter, and the fineness of the p.u.l parameters' model. This model is incompatible with cables whose lengths exceed tens of meters. Indeed, the simulation time depends strongly on the number of nodes.
Reference [10] proposes a solution based on the determination of the admittance matrix from the simulation of an equivalent cascaded cell model.

In this context, the aim of this article is to propose a simple and efficient method of reduced modeling of power cables in the time domain. The developed method must respect the requirements of stability, speed and precision.
Circuit type models are considered the most suitable for the study of conducted electromagnetic disturbances. To obtain a cable model of this type we have chosen the VHDL-AMS language. It allows to insert directly the differential equations and to manipulate quantities of different physical natures. In addition, it is a powerful means of modeling [11]. ANSYS Simplorer is the most suitable VHDL-AMS simulator.

The remainder of this article is organized as follows:
Section II presents the three wire shielded energy cable that is the subject of this study. The third section describes the adopted modeling method. While Section IV demonstrates the validity of our approach in both frequency and time domains. After that, Section V gives a simulation example of a motor drive system fed by the proposed cable model. A filtering solution has been used to mitigate the level of overvoltage spikes. Finally, we end with a conclusion.

Ali Krim is with Signals Systems and Components Laboratory (SSCL), Faculty of Sciences and Technologies USMBA, BP. 2202, Fez, Morocco. Email: ali.krim@usmba.ac.ma.

Abderazzak Lakrim with Signals Systems and Components Laboratory (SSCL), Faculty of Sciences and Technologies USMBA, BP. 2202, Fez, Morocco. Email: abderrazak.lakrim@usmba.ac.ma.

Driss Tahri is with Signals Systems and Components Laboratory (SSCL), Faculty of Sciences and Technologies USMBA, BP. 2202, Fez, Morocco. Email : idriss_tahri@yahoo.fr.

II. THREE-WIRE SHIELDED POWER CABLE

The geometric characteristics of the cable under study are shown in Fig 1. The cable is assumed uniform. The self and mutual impedances of the shield and the coupling between the conductors have been taken into account.

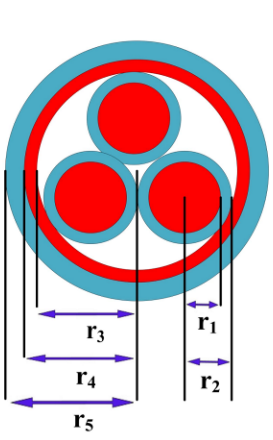

r_1	0.69 mm
r_2	1.155 mm
r_3	2.59 mm
r_4	2.7 mm
r_5	3.2 mm
σ_0	46 MS/m
ε_r	4.4

Fig. 1 Geometrical characteristics of the power cable.

When the propagation of the electromagnetic waves in the cable is in TEM (Transverse Electromagnetic) or quasi-TEM mode, the frequency behavior of this one is governed by the equations of the telegraphists:

$$\frac{\partial U(s,x)}{\partial x} = -\left(R(s)+s.L(s)\right).I(s,x) \quad (1)$$

$$\frac{\partial I(s,x)}{\partial x} = -\left(G(s)+s.C(s)\right).U(s,x) \quad (2)$$

With S is the Laplace operator. R, L, G and C are respectively the p.u.l resistance, inductance, conductance and capacitance matrices. $U(x,s)$ and $I(x,s)$ are the voltage vector and the current vector at the position x.

The resolution of these coupled equations (1) and (2) in the frequency domain makes it possible to find the relationship between the cable's input and output parameters [6]:

$$\begin{pmatrix} I_e \\ -I_s \end{pmatrix} = \hat{Y}.\begin{pmatrix} U_e \\ U_s \end{pmatrix} \quad (3)$$

where:

$$\hat{Y} = \begin{pmatrix} \hat{Y}_s & \hat{Y}_M \\ \hat{Y}_M & \hat{Y}_s \end{pmatrix} \quad (4)$$

Equation (3) is the multiport admittance model of the cable where:

$$\hat{Y}_M = -\sqrt{Y.Z^{-1}}.\left(\sinh\left(d.\sqrt{Y.Z}\right)\right)^{-1} \quad (5)$$

$$\hat{Y}_s = -\hat{Y}_M.\cosh\left(d.\sqrt{Y.Z}\right) \quad (6)$$

With $Z = R + sL$ is the cable per unit length longitudinal impedance matrix while $Y = G + sC$ is the cable per unit length admittance matrix. The parameter d represents the cable length. U_e, I_e, U_s and I_s respectively denote the voltage and current vectors at the cable input and output. The shield is chosen as a voltage reference.

Given the configuration of the cable (Fig. 1), one can notice its rotational symmetry. This property simplifies the modeling procedure. The p.u.l admittance and impedance matrices are circulant and symmetric. These class of matrices in general have very interesting properties:

- The product, the sum and the inverse of two symmetric circulant matrices is a symmetric circulant matrix.
- The product is commutative.
- Symmetric circulant matrices of order 3 are diagonalizable in the same base. In addition, the common diagonalization matrix is real.

Consequently, $\hat{Y}_s$ the cable proper admittance and $\hat{Y}_M$ the cable mutual admittance are symmetric circulant matrices. Because of the last property, instead of modeling all admittance matrix coefficients, it is enough to focus on its eigenvalues. The p.u.l impedance matrix can be written in the following form:

$$Z = \begin{pmatrix} Z_{11} & Z_{12} & Z_{12} \\ Z_{12} & Z_{11} & Z_{12} \\ Z_{12} & Z_{12} & Z_{11} \end{pmatrix} \quad (7)$$

With Z_{ij} are complex numbers. After diagonalization of the matrix Z we obtain:

$$Z = V.Z_d.V^{-1} \quad (8)$$

Where:

$$V = \begin{pmatrix} -1 & -1 & 1 \\ 1 & 0 & 1 \\ 0 & 1 & 1 \end{pmatrix} \quad (9)$$

$$Z_d = \begin{pmatrix} Z_{11}-Z_{12} & 0 & 0 \\ 0 & Z_{11}-Z_{12} & 0 \\ 0 & 0 & Z_{11}+2.Z_{12} \end{pmatrix} \quad (10)$$

Equation (9) gives a particular form of the eigenvectors' matrix. Generally, the matrix V can have multiple forms. We proceed in the same way to diagonalize the p.u.l admittance matrix.

Based on the diagonalization of a three-order symmetric circulant matrix and taking advantage of the admittance matrix form (4). One can deduce the following transformation matrix:

$$T = \begin{pmatrix} V & V \\ V & -V \end{pmatrix} \quad (11)$$

After replacement, (3) can be written as follows:

$$\begin{pmatrix} I_e \\ -I_s \end{pmatrix} = T\,\tilde{Y}\,T^{-1}.\begin{pmatrix} U_e \\ U_s \end{pmatrix} \quad (12)$$

where $\tilde{Y} = diag(\tilde{Y_1},\tilde{Y_2},\tilde{Y_3},\tilde{Y_4},\tilde{Y_5},\tilde{Y_6})$. With $\tilde{Y_1} = \tilde{Y_2}$ and $\tilde{Y_5} = \tilde{Y_4}$.

From (11), we can deduce the expression of the inverse of T:

$$T^{-1} = \frac{1}{2}\begin{pmatrix} V^{-1} & V^{-1} \\ V^{-1} & -V^{-1} \end{pmatrix} \quad (13)$$

Replacing (13) in (12) leads to the following equation:

$$I_m^i = \tilde{Y}_i . U_m^i \quad (14)$$

For $i = 1, 2, ..., 6$, I_m^i and V_m^i are respectively the modal current and the modal voltage.

With:

$$\begin{cases} I_m^1 = \left(2.I_e^2 - I_e^1 - I_e^3 - I_s^1 + 2.I_s^2 - I_s^3\right)/6 \\ I_m^2 = \left(2.I_e^3 - I_e^2 - I_e^1 - I_s^1 - I_s^2 + 2.I_s^3\right)/6 \\ I_m^3 = \left(I_e^1 + I_e^2 + I_e^3 + I_s^1 + I_s^2 + I_s^3\right)/6 \\ I_m^4 = \left(2.I_e^2 - I_e^1 - I_e^3 + I_s^1 - 2.I_s^2 + I_s^3\right)/6 \\ I_m^5 = \left(2.I_e^3 - I_e^2 - I_e^1 + I_s^1 + I_s^2 - 2.I_s^3\right)/6 \\ I_m^6 = \left(I_e^1 + I_e^2 + I_e^3 - I_s^1 - I_s^2 - I_s^3\right)/6 \end{cases} \quad (15)$$

$$\begin{cases} U_m^1 = \left(2.U_e^2 - U_e^1 - U_e^3 - U_s^1 + 2.U_s^2 - U_s^3\right)/6 \\ U_m^2 = \left(2.U_e^3 - U_e^2 - U_e^1 - U_s^1 - U_s^2 + 2.U_s^3\right)/6 \\ U_m^3 = \left(U_e^1 + U_e^2 + U_e^3 + U_s^1 + U_s^2 + U_s^3\right)/6 \\ U_m^4 = \left(2.U_e^2 - U_e^1 - U_e^3 + U_s^1 - 2.U_s^2 + U_s^3\right)/6 \\ U_m^5 = \left(2.U_e^3 - U_e^2 - U_e^1 + U_s^1 + U_s^2 - 2.U_s^3\right)/6 \\ U_m^6 = \left(U_e^1 + U_e^2 + U_e^3 - U_s^1 - U_s^2 - U_s^3\right)/6 \end{cases} \quad (16)$$

Equation systems (15) and (16) can be implemented directly in the Simplorer software by using VHDL-AMS language. Thanks to these equations, we establish the connection block that connects the voltages and the currents at the cable input and the output with modal voltages and currents. The next step is to find a time domain representation of the admittance matrix eigenvalues in order to develop the overall cable model.

III. Vector Fitting

The vector fitting technique [12]-[13] and [14] has been widely used to model the frequency behavior of electrical systems [15]. It is a very attractive macro-modeling method. Among its advantages, we mention the simplicity of converting the frequency domain model into a time domain one by using differential equations or the convolution product. In addition, one can generate the equivalent electrical circuit based on RLC component. Because of the efficiency of this technique, we will apply it on our matrix.

The result obtained by applying this method must verify the criteria of causality, stability and passivity [16]-[17]. The estimated admittance matrix satisfies these criteria if its eigenvalues have a positive real part and their poles are in the left part of the complex plane. The eigenvalues of the admittance matrix are approximated as follows:

$$\tilde{Y}_i(s) \approx \sum_{k=1}^{N_a^i} \frac{r_k^i}{s - p_k^i} + d_i \quad (17)$$

The coefficients r_k^i and p_k^i are respectively the residues and the poles of the ith eigenvalue, and d_i is a real coefficient while N_a^i is the approximation order. Replacing (17) in (14) yields:

$$I_m^i = \sum_{k=1}^{N_i} I_k^i + d_i . U_m^i \quad (18)$$

If r_k^i and p_k^i are real we have:

$$I_k^i = \frac{r_k^i}{s - p_k^i} . U_k^i \quad (19)$$

In the case where r_k^i and p_k^i are complex numbers we obtain:

$$I_k^i = \left(\frac{r_k^i}{s - p_k^i} + \frac{\overline{r}_k^i}{s - \overline{p}_k^i}\right).U_k^i \quad (20)$$

$$N_i = N_r^i + \frac{N_c^i}{2} \quad (21)$$

With the coefficients N_r^i and N_c^i denotes respectively the number of real poles and the number of complex poles. $\tilde{Y}_i$ may be implemented in the Simplorer software by paralleling $N_i + 1$ dipoles such as:

- A dipole described as follows:

$$I = d_i . U \quad (22)$$

- N_r^i dipoles characterized by the following differential equation:

$$\frac{dI}{dt} - p_k^i . I = r_k^i . U \quad (23)$$

- $N_c^i / 2$ dipoles described in the time domain by the following second-order differential equation:

$$\frac{d^2I}{dt^2} - 2.\mathrm{Re}(p_k^i).\frac{dI}{dt} + \left|p_k^i\right|^2.I = 2.\mathrm{Re}(r_k^i).\frac{dU}{dt} - 2.\mathrm{Re}(r_k^i.\overline{p}_k^i).U \quad (24)$$

With U is the voltage across the dipole terminals while I is the current flowing through it. Thus, the cable macro-model is obtained by connecting these dipoles with the connection block terminals, which correspond to the modal parameters (current and voltage). Whenever the cable length is changed the modeling procedure must be run again. It should be noted that the longer the cable is, the more the number of dipoles would increase.

IV. Simulation and Validation

In this section, by applying the proposed modeling procedure, we simulate the cable described in figure 1, in both the time and the frequency domains. We validate our proposal against the responses of the well-established cascaded cell model. These are the steps to build up the reduced cable model:

- Computation of the per unit length parameters.
- Extraction of the cable admittance matrix.
- Diagonalization of the admittance matrix.
- Vector fitting of the admittance matrix eigenvalues.
- Passivity enforcement of the rational model.
- Construction of dipoles and connection block.

A. The cable p.u.l parameters.

The p.u.l impedance matrix has two distinct coefficients: the self-impedance of each conductor and the mutual impedance between two conductors. We used ANSYS Q3D Extractor to estimate the frequency domain evolution of the cable p.u.l parameters in the frequency range [100 KHz, 30 MHz]. These will help us to calculate the equivalent admittance matrix of the cable.

Fig. 2 shows the evolution of the self-resistance R_{11} and the mutual resistance R_{12} over the frequency range under consideration. On the other hand, Fig. 3 describes the variation of the p.u.l inductances. This variation is due to the skin and proximity effects. In most cases, the p.u.l capacitances are considered constant [5, 17], and the p.u.l conductances are neglected. Considering these parameters will slightly influences the model's results. Generally, the procedure described above still applies. Because we are interested in the equivalent admittance matrix.
Tab. 1 summarizes the values adopted in this simulation.

TABLE I
Values of the PUL admittance matrix coefficients

Coefficients	Values	Coefficients	Values
G_{11}	1,9. 10^{-05} S	C_{11}	1,85554.10^{-10} F
G_{12}	5. 10^{-06} S	C_{12}	3,7804. 10^{-11} F

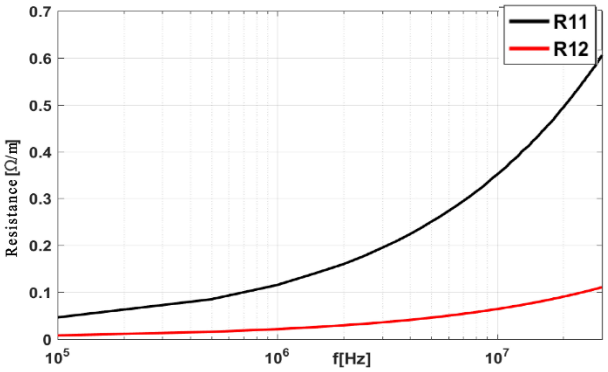

Fig. 2. The frequency evolution of the cable PUL resistances

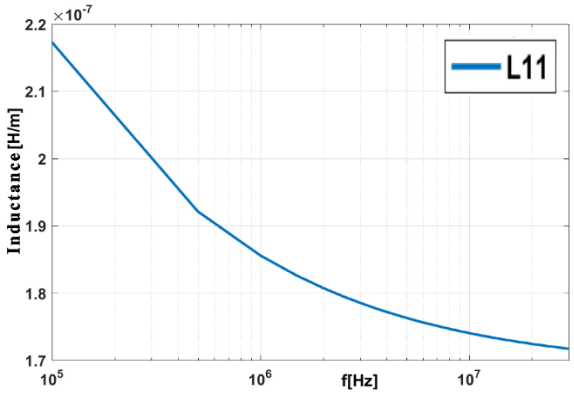

(a)

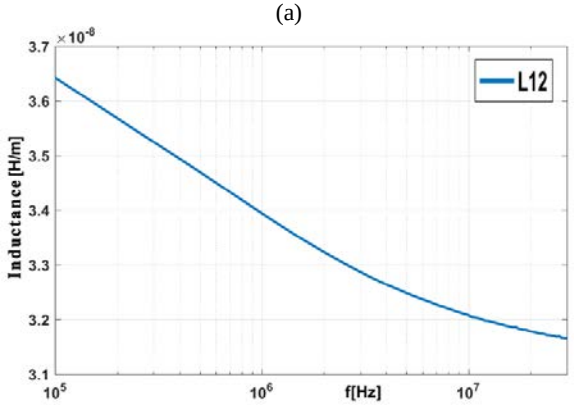

(b)

Fig. 3. The frequency evolution of the cable PUL: (a) self-inductance, (b) mutual inductance.

Once these curves are obtained (Fig. 2 and Fig. 3), we proceed as described in section III. Rational models can be computed under MATLAB by using the Matrix fitting toolbox.

B. Vector fitting of the admittance matrix eigenvalues.

In this subsection, we establish a comparison between the original model and the passive one. The later has been obtained after the enforcement of the passivity of the rational model computed by vector fitting technique. Fig. 4 and Fig. 5 show that the two models are in good agreement and fit each other accordingly in the selected frequency range. This results demonstrates the high performances and precision of the vector fitting technique.

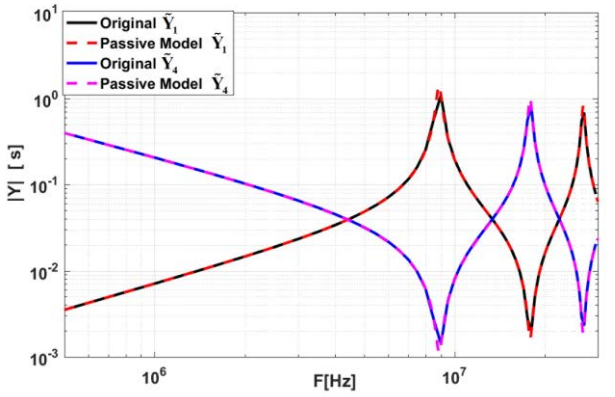

(a)

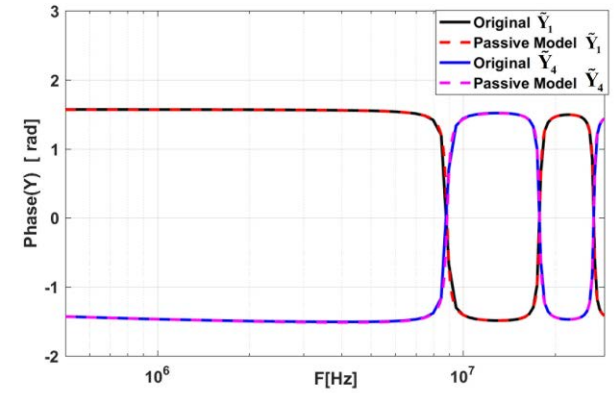

(b)

Fig.4 Comparison between the original and the passive model of $\tilde{Y}_1$ and $\tilde{Y}_4$: (a) module, (b) phase.

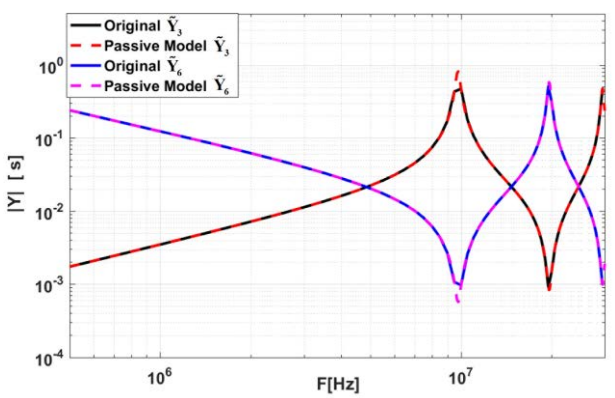

(a)

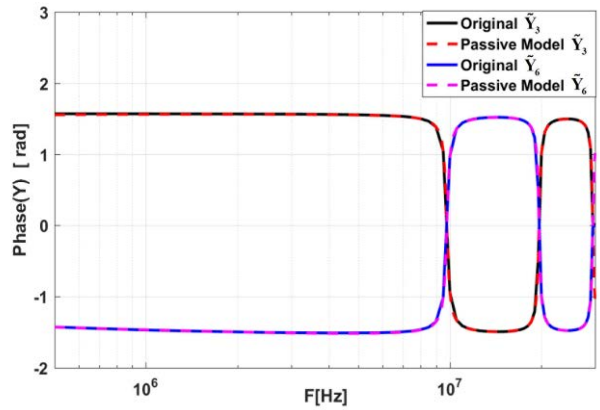

(b)

Fig.5 Comparison between the original and the passive model of $\tilde{Y}_3$ and $\tilde{Y}_6$: (a) module, (b) phase.

C. Validation of the reduced cable model in the frequency domain.

To validate our method in the frequency domain. We proceed by a simulation of the proposed model and the cascaded cells one in common mode for both short-circuit and open-circuit tests. The chosen cable length is equal to 10m and the frequency band is from 100 KHz to 30MHz. Fig. 6 compares the simulated values of the two models. The curves obtained coincide perfectly over the entire predefined frequency range. This attests the validity of our approach. In addition, our model is simpler.

D. Validation of the cable model in the time domain

Fig. 7 shows the simulation setup used to validate the reduced cable model in the time domain. The generator delivers a trapezoidal signal, the signal's rise and fall time are equal ($t_r = t_f = 20ns$).

Fig. 8 shows the comparison of the time response of the reduced cable model with that of the cascaded cell model. The results of this simulation are very satisfactory. Our model is both simple and precise. In addition, the simulation time is very short. Indeed, the simulation time is 4 seconds while that of the cascaded cell model is 5 minutes and 44 seconds. This simulation was done on a PC with 2.4 GHz CPU and 4GB of RAM.

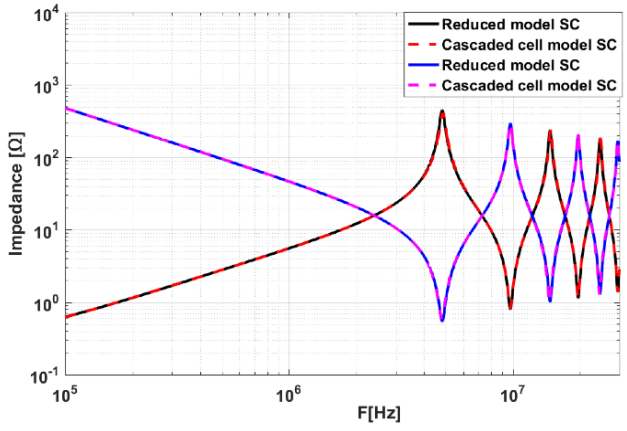

Fig. 6. The frequency evolution of the cable impedance module in common mode for Short Circuit (SC) and Open Circuit (OC) tests.

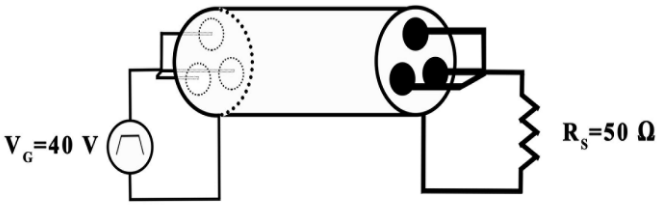

Fig. 7. The simulation setup for time domain analysis.

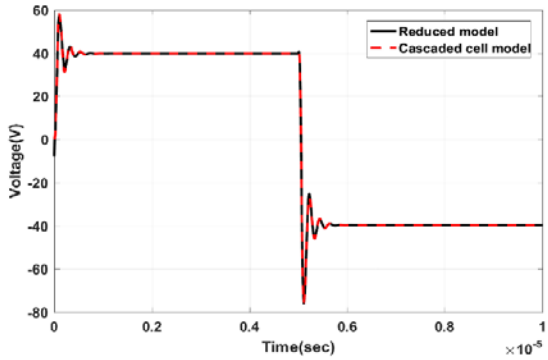

Fig. 8. The voltage across the resistor R_s.

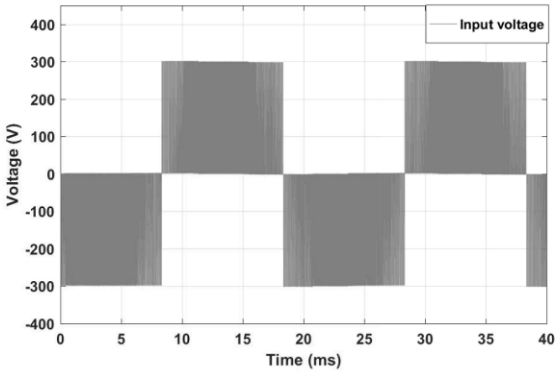

Fig. 9. The waveform of the voltage at cable input.

V. Application Example

In this section of this work, an application example that consists of a motor drive system fed by a long power cable is handled in ANSYS Simplorer software. Two simulations have been performed. The first one considers the system without any filtering solution. While the second introduces a passive filter to suppress the overvoltage spikes.

The simulation setup is described in Fig. 10. The design methodology of the filter RL-plus-C used during the second simulation has been explained in detail in [18]. Tab. 2 summarizes the components values of the filter.

TABLE II
VALUES OF THE FILTER PARAMETERS

Parameters	Values
R_f	49 Ω
L_f	670 µH
C_f	7.5 nF

The input voltage V_{DC} is 300 V and the switching frequency of the inverter f_s is set 10 KHz. Moreover, we used 50 meters cable length modeled as described in the previous sections.

Fig. 9 shows the voltage waveform at the cable inputs terminals. When the cable effect is neglected, the voltage at the motor terminals will be approximately the same. Fig. 11(a) depicts the overvoltage spikes that occurs when the cable model is inserted between the inverter and the motor. It is noticed that the magnitude of the voltage peaks at the cable outputs reaches 506 V (Fig. 12(a)). The increasing of the cable length will considerably increase these peaks.

Fig. 11(b) shows the waveform of the voltage at the motor terminals after the use of the filter mentioned before. It is noticed that the overvoltage spikes have been mitigated. The magnitude of the voltage peaks at the cable outputs does not exceed 358 V (Fig. 12(b)).

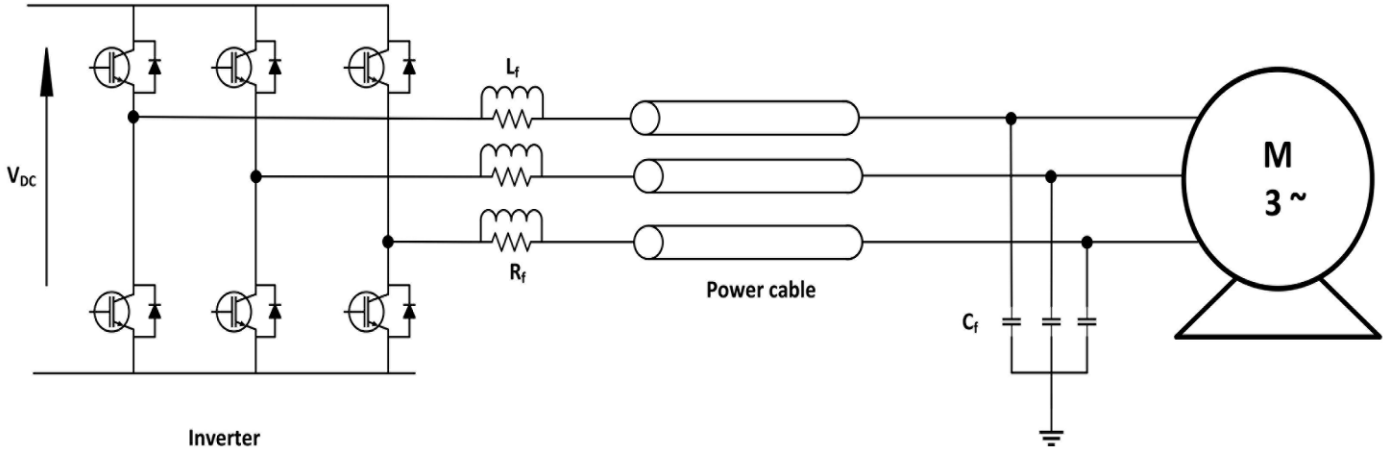

Fig. 10. Circuit schematic of the simulation setup.

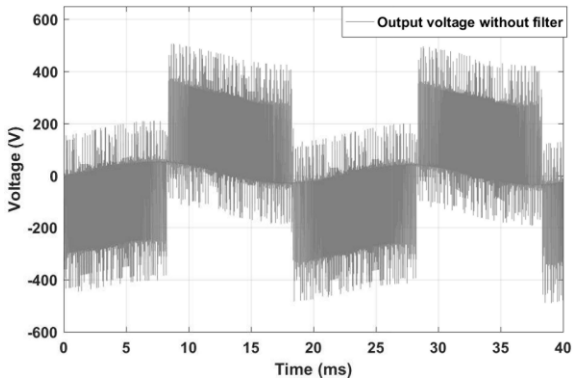

(a)

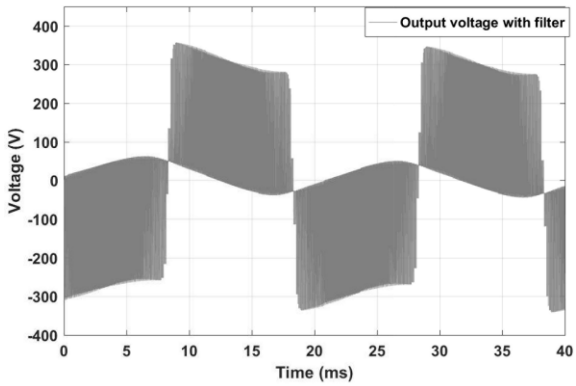

(b)

Fig. 11. The waveform of the voltage at cable output: (a) without filter, (b) with filter.

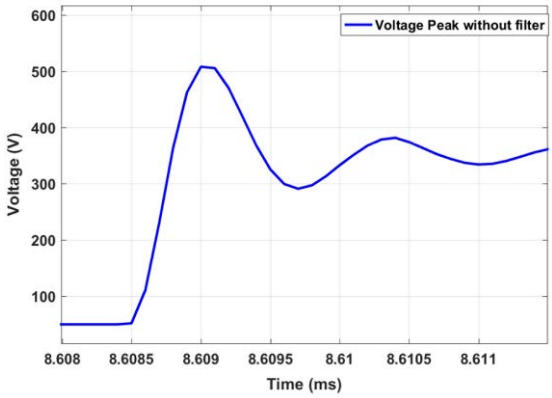

(a)

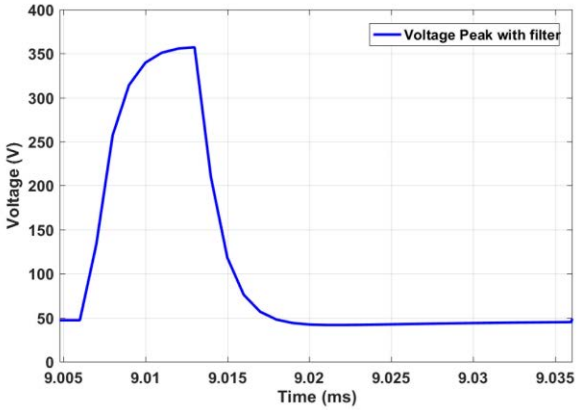

(b)

Fig. 12. The peak of the voltage at the motor terminals: (a) without filter, (b) with filter.

VI. Conclusion

In this paper, we propose a behavioral model of three-wire shielded power cables. Based on the results of the transmission line theory and calculating the cable p.u.l impedance and p.u.l admittance matrices, the equivalent admittance matrix can be derived for any cable length. Modal transformation reduces the complexity of the model. Indeed, instead of approximating a whole frequency dependent matrix, the problem remains to model the four distinct eigenvalues. Then, using the vector-fitting tool, we obtain a model that is easy to implement in the Simplorer simulator. Finally, the simulations made for a length of 10 meters validate the proposed method in the frequency and time domains. Our method has several advantages among them:

- Simple.
- takes into account the frequency dependence of the cable parameters.
- Treatment of long cables with a very low computational time.
- This method can also model the four-wire shielded power cables.

References

[1] Xiangyu Lu, Shuxue Zhang, Chen Liu, Pengkang Xie and Henglin Chen, "Modeling of common-mode current in motor cable of inverter-fed motor drive system," *2016 Asia-Pacific International Symposium on Electromagnetic Compatibility (APEMC)*, Shenzhen, 2016, pp. 511-514.

[2] L. Wang, C. Ngai-Man Ho, F. Canales and J. Jatskevich, "High-Frequency Modeling of the Long-Cable-Fed Induction Motor Drive System Using TLM Approach for Predicting Overvoltage Transients," in *IEEE Transactions on Power Electronics*, vol. 25, no. 10, pp. 2653-2664, Oct. 2010.

[3] A. Krim, D. Tahri and A. Lakrim, "VHDL-AMS based frequency domain model of four-wire shielded energy cable," *2018 19th IEEE Mediterranean Electrotechnical Conference (MELECON)*, Marrakech, 2018, pp. 144-148.

[4] C. G. Kaloudas, A. I. Chrysochos and G. K. Papagiannis, "FDTD analysis of multiphase power cable systems using distributed constant parameters," *MedPower 2014*, Athens, 2014, pp. 1-8.

[5] N. Idir and Y. Weens and M. Moreau and J. J. Franchaud, "High-Frequency Behavior Models of AC Motors", *IEEE Tran. On Magnetics*, Vol: 45, No.1, pp. 133 – 13, Jan. 2009.

[6] C. Paul, Analysis of Multi-Conductor Transmission Line. New York: Wiley, 2008.

[7] U. R. Patel and P. Triverio, "Skin Effect Modeling in Conductors of Arbitrary Shape Through a Surface Admittance Operator and the Contour Integral Method," in *IEEE Transactions on Microwave Theory and Techniques*, vol. 64, no. 9, pp. 2708-2717, Sept. 2016.

[8] V. D. Santos, N. Roux, B. Revol, B. Sareni, B. Cougo and J. Carayon, "Unshielded cable modeling for conducted emissions issues in electrical power drive systems," *2017 International Symposium on Electromagnetic Compatibility - EMC EUROPE*, Angers, 2017, pp. 1-6

[9] N. Y. Abed and O. A. Mohammed, "Frequency-Dependent Coupled Field-Circuit Modeling of Armored Power Cables Using Finite Elements," in *IEEE Transactions on Magnetics*, vol. 47, no. 5, pp. 930-933, May 2011.

[10] Y. Huangfu, L. Di Rienzo and S. Wang, "Frequency-Dependent Multi-Conductor Transmission Line Model for Shielded Power Cables Considering Geometrical Dissymmetry," in *IEEE Transactions on Magnetics*, vol. 54, no. 3, pp. 1-4, March 2018.

[11] L. Göhler and M. Rose, "A comprehensive physics-based power MOSFET model in VHDL-AMS for circuit simulations," *Proceedings of the 2011 14th European Conference on Power Electronics and Applications*, Birmingham, 2011, pp. 1-9.

[12] B. Gustavsen and A. Semlyen, "Rational approximation of frequency domain responses by Vector Fitting", *IEEE Trans. Power Delivery*, vol. 14, no. 3, pp. 1052-1061, July 1999.

[13] B. Gustavsen, "Improving the pole relocating properties of vector fitting", *IEEE Trans. Power Delivery*, vol. 21, no. 3, pp. 1587-1592, July 2006.

[14] D. Deschrijver, M. Mrozowski, T. Dhaene, and D. De Zutter, "Macromodeling of Multiport Systems Using a Fast Implementation of the Vector Fitting Method", *IEEE Microwave and Wireless Components Letters*, vol. 18, no. 6, pp. 383-385, June 2008.

[15] Y.-M. Yang, H.-M. Peng, and Q.-D. Wang, "Common model EMI prediction in motor drive system for electric vehicle application," *J. Electr. Eng. Technol*., vol. 10, pp. 205–214, Jan. 2015.

[16] A. Semlyen and B. Gustavsen, "A half-size singularity test matrix for fast and reliable passivity assessment of rational models", *IEEE Trans. Power Delivery*, vol. 24, no. 1, pp. 345-351, January 2009.

[17] B. Gustavsen, "Fast passivity enforcement for pole-residue models by perturbation of residue matrix eigenvalues", *IEEE Trans. Power Delivery*, vol. 23, no. 4, pp. 2278-2285, Oct 2008.

[18] K. K. Yuen and H. S. Chung, "A Low-Loss "RL-Plus-C" Filter for Overvoltage Suppression in Inverter-Fed Drive System With Long Motor Cable," in *IEEE Transactions on Power Electronics*, vol. 30, no. 4, pp. 2167-2181, April 2015.

Ali KRIM received the Eng. Degree from Faculty of sciences and technologies of FEZ, Morocco in 2016. He is currently pursuing a PhD (Power electronics). His current research interest includes electromagnetic compatibility in power drive systems.

Abderrazak LAKRIM received the Master Degree from university of Sidi Mohamed Ben Abdellah of FEZ, Morocco in 2010. He received the PhD degree in Power electronics from the same university in 2016. His current research interest includes design and modeling of power transistors and electro-magnetic compatibility in the power chain.

Driss TAHRI received the PhD degree in Power Electronics from the University BLAISE PASCAL of CLERMONT FERRAND, France, in 1994. Since 1995, he has been a professor at the faculty of science and technology-Fes, MOROCCO (FST-FES). His research interest includes Power Electronics and electromagnetic compatibility (EMC). He was at the head of the EMC unit within the Laboratory of signals, systems and components (LSSC) at the FST-Fez (Morocco).